Disrupted hypothalamo-pituitary axis in association with reduced SHH underlies the pathogenesis of NOTCH-deficiency

Houda Hamdi-Roze, Michelle Ware, Hélène Guyodo, Aurélie Rizzo, Leslie Ratié, Maïlys Rupin, Wilfrid Carré, Artem Kim, Sylvie Odent, Christèle Dubourg, et al.

Disrupted hypothalamo-pituitary axis in association with reduced SHH underlies the pathogenesis of NOTCH-deficiency

Houda Hamdi-Rozé[1,2], Michelle Ware[1], Hélène Guyodo[1], Aurélie Rizzo[1], Leslie Ratié[1], Maïlys Rupin[1], Wilfrid Carré[1,2], Artem Kim[1], Sylvie Odent[1,3], Christèle Dubourg[1,2], Véronique David[1], Marie de Tayrac[1,2]and Valérie Dupé[1] *

[1]Univ Rennes, CNRS, IGDR -Institut de Génétique et Développement de Rennes - UMR6290, F-35000, Rennes, France

[2]Service de Génétique Moléculaire et Génomique, CHU, Rennes F-35033, France

[3]Service de Génétique Clinique, CHU, Rennes, France.

*Corresponding author: Valérie Dupé, Institut de Génétique et Développement de Rennes, Faculté de Médecine, CNRS UMR6290, Université de Rennes 1, IFR140 GFAS, 2 Avenue du Pr. Léon Bernard, 35043 Rennes Cedex, France

E-mail: valerie.dupe@univ-rennes1.fr

Context: In human, Sonic Hedgehog, SHH, haploinsufficiency is the predominant cause of holoprosencephaly, a structural malformation of the forebrain midline characterised by phenotypic heterogeneity and incomplete penetrance. The NOTCH signalling pathway has recently been associated with holoprosencephaly, in humans, but the precise mechanism involving NOTCH signalling during early brain development remains unknown.

Objective: The aim of this study was to evaluate the relationship between SHH and NOTCH signalling in order to determine the mechanism by which NOTCH dysfunction could cause midline malformations of the forebrain.

Design: In this study, we have used a chemical inhibition approach in the chick model and a genetic approach in the mouse model. We reported results obtained from clinical diagnosis of a cohort composed of 141 holoprosencephaly patients.

Results: We demonstrated that inhibition of NOTCH signalling in chick embryos as well as in mouse embryos induces a specific downregulation of SHH in the anterior hypothalamus. Our data in the mouse also revealed that the pituitary gland was the most sensitive tissue to *Shh* insufficiency and that haploinsufficiency of the SHH and NOTCH signalling pathways synergized to produce a malformed pituitary gland. Analysis of a large holoprosencephaly cohort revealed that some patients possessed multiple heterozygous mutations in several regulators of both pathways.

Conclusions: These results provided new insights into molecular mechanisms underlying the extreme phenotypic variability observed in human holoprosencephaly. They showed how haploinsufficiency of the SHH and NOTCH activity could contribute to specific congenital hypopituitarism that was associated with a *sella turcica* defect.

Keywords: SHH, NOTCH, Holoprosencephaly, Hypothalamus, brain development, rare disease.

Introduction

The development of the vertebrate brain is complex and requires a tightly controlled spatial and temporal orchestration of numerous signalling pathways. Among these pathways is Sonic Hedgehog (SHH), an essential morphogenetic signal dictating cell fate decisions during early forebrain development (1). Both embryological evidence in chick and genetic evidence in mouse have shown that SHH secreted by the axial mesoderm underlying the neural plate initiates development of the ventral midline (2, 3). SHH then induces expression of itself in the ventral midline of the developing forebrain, which will become the hypothalamus primordium. Subsequently, during hypothalamic patterning, SHH also acts as a local signal to subdivide the developing hypothalamus into subregions (4, 5). From rostral to caudal regions, the presumptive hypothalamus can be subdivided into three regions, the anterior, the tuberal and the mammillary hypothalamus. The anterior hypothalamus is the first region to produce differentiated neurons giving rise to the tract of the postoptic commissure (6). Each hypothalamic region has distinct patches of nuclei and SHH signalling is essential for the differentiation of these resident neurons (7, 8). In addition, recent advances have shown, in both the chick and mouse brains, that SHH produced in the hypothalamus is essential for the development of the infundibulum and Rathke's pouch that will form the pituitary gland (9-11). Therefore, accurate regulation of *Shh* expression is crucial to pattern the ventral region of the brain as well as the anterior pituitary gland (8, 10).

Consistent with its fundamental role during development, *SHH* haploinsufficiency account for 15 % of the molecularly diagnosed cases of holoprosencephaly (HPE) (12). This human structural brain malformation results in a graduated malformation of the forebrain. The most severe forms of HPE are characterised by the failure of the cerebral hemispheres and the optic vesicles to separate into bilateral structures (13). *SHH* haploinsufficiency can also contribute to less severe phenotypes such as microcephaly, hypothalamic-dysfunction, pituitary insufficiency with moderate facial disorders like hypotelorism (abnormally close-set eyes) or having only a single median incisor (14, 15). Only these

mild forms of HPE are compatible with life (16). Genetic research on HPE patients and their families over the past two decades has implicated other signalling pathways in the disease such as FGF, NODAL and NOTCH (17-20). NODAL and FGF are known to act in the pathology of HPE by regulation of SHH activity (1). The exact mechanism by which NOTCH dysfunction could cause HPE-like phenotypes is unexplained (18, 21).

NOTCH signalling is an important evolutionary conserved mechanism known to control cell fates through local interactions. This pathway utilises a membrane bound ligand that when in contact with a receptor leads to the release of a cytoplasmic fragment of the receptor, which forms a complex with the transcriptional regulator RBPJ (Recombination signal binding protein for immunoglobulin kappa J). This complex is then capable of transcriptional regulation (22). Early in development, NOTCH is implicated in the correct patterning of the first neuronal population of the developing hypothalamus (23, 24). Colocalisation of SHH activity and NOTCH components, such as *Dll1* and *Hes5*, in both chick and mouse embryos is present at the level of the developing ventral forebrain corresponding to the hypothalamus primordium (23-25).

This study focuses on a unique aspect of canonical NOTCH function in the developing anterior hypothalamus. Using chick and mouse embryonic models, we demonstrate that embryos lacking NOTCH activity during early forebrain development exhibit a specific reduction of SHH signalling in the anterior hypothalamus. This leads to a phenotype that is reminiscent to an inactivation of *Shh* in this tissue. These data demonstrate that the NOTCH pathway is implicated in the etiology of HPE through the regulation of *Shh* expression and, thus contributes to the phenotypic heterogeneity that is observed in HPE patients.

Materials and Methods

Generation of mouse lines and genetic crosses

To generate conditional *Rbpj* knock-out mice, *Rbpj*$^{L/L}$ (26) mice were crossed with *R26RCreER*^{T2} (27) mice to generate *Rbpj*$^{L/L}$*;CreER*$^{T2+/-}$. *Rbpj*$^{L/L}$*;R26RmTmG*$^{+/+}$ mice (28) were crossed with *Rbpj*$^{L/L}$*;CreER* $^{T2+/-}$ mice to evaluate Cre-mediated excision (Fig. S4; (29). To activate Cre recombinase, tamoxifen (Sigma) was dissolved in sunflower oil at a concentration of 10 mg/ml. Tamoxifen (4 mg) or a vehicle was injected intraperitoneally (IP) between embryonic day (E) 7.75 and E8.0. Embryos were harvested between E9.5 and E11.5. *Rbpj*$^{+/-}$ (gift from Dr. Tasuku Honjo) and *Shh*$^{+/-}$ mice (Jackson Laboratories, Bar Arbor, ME, USA) have been described previously (2, 30). Embryos and mice were genotyped by PCR on DNA samples prepared from tail tips, yolk sacs or whole embryos. Primer sequences and PCR protocols are available on request. The mice were maintained in a room with controlled temperature (21-22°C) under a 12-12 light-dark cycle (light cycle from 7:00 to 19:00) with ad libitum access to the food and water.

Chick embryos and *ex ovo* roller culture

Fertilised chicken (*Gallus gallus*) eggs were obtained from E.A.R.L. Les Bruyères (France). Eggs were incubated in a humidified incubator at 38˚C until the required developmental stages described according to Hamburger and Hamilton (31).

For *ex ovo* roller culture, embryos were collected at HH9 and cultured as described previously (32). Loss of function experiments were performed with the γ-secretase inhibitor DAPT (Sigma, France), a chemical that inhibits NOTCH signalling *in vitro*, dissolved in DMSO. Embryos were treated with 40 µM of DAPT in L15 culture medium, supplemented with chick serum. As a control, embryos were treated with DMSO.

In situ hybridisation

All embryos were fixed in 4% PFA/PBS at 4˚C overnight, rinsed and processed for whole-mount RNA *in situ* hybridisation. Sense and anti-sense probes were generated from plasmids cloned as previously described (24) or plasmids provided as a gift. The protocol for single and double *in situ* hybridisation has been previously described (23). For double labelling, Digoxigenin and Fluorescein labelled probes were incubated together. The Digoxigenin antibody (Roche) was added first, followed by the NBT/BCIP reaction. After inactivation of the colour reaction, the embryos were fixed with 4% PFA overnight, then the Fluorescein antibody (Roche) was added, followed by fast red reaction (VectorRed).

Histology and Skeletal preparation

For histology, E18.5 embryos were fixed in Bouin's fluid for 7 days, embedded in paraffin, serially sectioned and stained with Haematoxylin eosin and safran. For skeletal preparation, E18.5 embryos were dissected, skinned and eviscerated. Subsequently, embryos were fixed in acetic acid/ethanol overnight and stained for four days in an Alcian Blue solution (Sigma; A3157). Any remaining tissue was digested in 1% potassium hydroxide and bones were then stained with Alizarin red (Sigma; A5533). Finally, embryos were cleared with progressively increasing concentrations of glycerol.

Ethics statement

All experiments with mice were carried out in accordance with the European Communities Council Directive of 24 November 1986. VD, as the principal investigator in this study, was granted the accreditation 35-123 to perform the reported experiments and the experimental procedures were authorised by the French Ministry of Research committee C2EA-07 under the protocol APAFIS#3532-2016010514029297.

HPE database sequencing and analysis

The cohort presented in this study is comprised of 141 patients diagnosed with HPE. The full retrospective cohort was constituted of all the cases referred to our laboratory for molecular diagnosis during a ten-year period (2017-2019) from eight French Centers Labeled for Developmental Anomalies (CLADs), centers of prenatal diagnosis and several European centers. Informed consent was obtained from all patients or legal representatives according to the protocols approved by the local ethics committee (Rennes Hospital - DC- 2015-2565). Samples were analysed by Next Generation Sequencing. Libraries were prepared using the Sure Select XT Focused exome® kit (Agilent Technologies), which covers 5504 genes associated with known phenotypes and Illumina sequencing solution on either HiSeq 1500® or NextSeq 550® (33). Data were analysed using our local bio-informatic pipeline including BWA MEM alignment (34), GATK/Free Bayes variant calling (35) and ANNOVAR (36) and ALAMUT (Interactive Biosoftware) annotations. A filter-based annotation identified variants and their associated frequency that were reported in different databases (dbSNP138, 1000-Genome, GnomAD). Exonic non-synonymous variants in genes belonging to NOTCH and SHH pathways were selected using a database frequency threshold of 0.01.

Results

Sonic hedgehog signalling was active in the presumptive hypothalamus before NOTCH activity in the chick embryo

To analyse the potential interaction between NOTCH and SHH signalling at the level of the developing hypothalamus, the chick was used as a model since molecular features defining the antero-posterior domains have been extensively described (10, 37). We first performed a detailed study of the expression of SHH effector target genes (*Nkx2.1* and *Ptch1*) and a NOTCH effector target gene (*Hes5*) (Fig. 1). It is well known that SHH signalling induces expression of *Nkx2.1* in the presumptive hypothalamus from HH8 (4-somites stage); making *Nkx2.1* the first marker that defines the hypothalamic progenitor state at HH8 (38). Expression of *Hes5*, a direct transcriptional target of NOTCH, has been considered a reliable readout of NOTCH signalling (23, 39).

To assess whether there was NOTCH activity when the hypothalamus tissue became *Nkx2.1*-positive, we performed double labelling of *Nkx2.1* and *Hes5* at HH9 (7 somite-stage) (Fig. 1A). This staining confirmed that *Hes5* was expressed in the midbrain at HH9, but not in the *Nkx2.1*-positive cells corresponding to the developing hypothalamus (Fig. 1A, bracket). This result indicated that SHH signalling was active in the early developing hypothalamus to induce *Nkx2.1* before NOTCH signalling was detected in the AH.

Overlapping activity of NOTCH and SHH signalling was restricted to the anterior hypothalamus

PTCH1, a SHH binding receptor, was upregulated at sites of active SHH signalling (40). In the chick brain, *Hes5* and *Ptch1* have their expression restricted in the anterior hypothalamus (AH) at stage HH13 (Ratié et al., 2013; Fu et al., 2017). To clarify further the timing of *Ptch1* and *Hes5* expression in the AH, we performed a more detailed expression analysis. At HH10 (10-somite stage), the first *Hes5* (Fig. 1B) and *Ptch1* (Fig. 1C) transcripts were expressed, at the level of the AH domain between the optic vesicles (OV). In agreement with the expression being located in the AH, at HH12 (16-somite stage), double labelling of *Nkx2.1* and *Hes5* showed that the expression of *Hes5* was confined within the anterior limit of *Nkx2.1* expression corresponding to the AH (Fig. 1D). This expression analysis revealed that NOTCH activity started at HH10 in the hypothalamus and the location of expression was restricted in the AH which also corresponded to the anterior limit of *Shh* expression at this stage (Fig. 1E; (37).

NOTCH activity maintained *Shh* expression in the chick anterior hypothalamus

We next investigated the potential interaction of NOTCH and SHH signalling during early differentiation of the AH. To address this, we used DAPT to inhibit NOTCH signalling and microarray analysis. After just 3 hours, this DAPT treatment caused a rapid downregulation of *Hes5* expression (23, 29).

As NOTCH activity was first detected in the hypothalamus at HH10, chick embryos were treated with DAPT from HH9 and harvested after 16 hours *ex ovo* roller culture, at approximately stage HH13. Microarray data was compared between DAPT-treated forebrains and DMSO-treated forebrains. DAPT treatment resulted in the differential expression of 1558 genes, with 769 genes upregulated and

789 genes downregulated (23). Interestingly, both *Shh* and *Ptch1* were significantly downregulated in DAPT-treated embryos compared to DMSO-treated embryos (Fig. S1; 29). This suggested that NOTCH signalling played a role in the regulation of SHH signalling during forebrain development.

To confirm this regulation, whole-mount *in situ* hybridisation was performed on chick embryos treated with DAPT. All DAPT-treated embryos (n=25) showed a consistent downregulation of *Shh* in the forebrain (Fig. 2A). When the neural tube was dissected this highlighted a highly specific downregulation of *Shh* in the AH and *Shh* expression was essentially normal, posteriorly, along the ventral neural tube (Fig. 2B). To examine the consequence of the loss of *Shh* in the AH domain of DAPT-treated embryos, we examined the expression of both *Nkx2.1* and *Ptch1*. In DAPT-treated embryos, *Ptch1* (n=11) expression was absent in the AH (Fig. 2C). *Nkx2.1* (n=9) expression was also lacking in the AH, but was still expressed in the tubero-mamillary hypothalamus (T-MH), although weaker compared to control embryos (Fig. 2D). From this expression analysis, we concluded that NOTCH signalling from HH10 was required to maintain *Shh* expression and the activity of its downstream target genes in the chick AH.

To show that the influence of NOTCH activity on hypothalamic development was time window-dependent the same *ex ovo* roller culture experiments were done with DAPT treatment at later embryonic stages. These data are shown in an online repository (Fig. S2; (29). The embryos treated with DAPT at HH10 gave similar results to the embryos treated at HH9, with no *Shh* expression in the AH. DAPT-treated embryos at HH11 gave a partial loss of *Shh* expression in the AH. There was no more effect on *Shh* expression in the AH when DAPT treatment took place after HH12 (data not shown). This temporal analysis of chick embryos with a loss of NOTCH function showed that NOTCH signalling maintained *Shh* expression and its activity in the AH was highly specific during a short time window between HH9 and HH12.

Inhibition of *Shh* expression and signalling in the ventral forebrain of *Rbpj*$^{-/-}$ mice

While our analysis using the chick embryo suggested an interaction between the SHH and NOTCH signalling pathways in the AH, we wanted to confirm this genetic interaction using the mouse model. To perturb NOTCH signalling we utilised a knockout allele of *Rbpj* (30), a common effector required for the activity of all four mammalian NOTCH receptors (41). *Rbpj* mutant mice are commonly used to study the role of NOTCH signalling, because inhibition of this transcriptional activator abrogates NOTCH signalling during development (39).

The expression of *Shh* and *Nkx2.1* was analysed by *in situ* hybridisation in these *Rbpj* null-mutants (*Rbpj*$^{-/-}$ embryos). At E9.0, the anterior limit of *Shh* expression corresponded to the AH (Fig. 3A; (42). At this stage, *Rbpj*$^{-/-}$ embryos (n=5) showed an overall downregulation of *Shh* expression along the neural tube (Fig. 3C), and *Shh* expression was completely absent in the AH from E9.0 (Fig. 3C, arrowhead).

The NOTCH pathway has been shown to be crucial for early cardiac development, therefore from E9.0, *Rbpj*$^{-/-}$ embryos suffered from a severe developmental delay (39, 42). Despite this delay, we managed to obtain *Rbpj*$^{-/-}$ embryos at E9.5 (n=3). In these embryos, *Nkx2.1* expression was completely absent in the AH (Fig. 3D, arrowhead) and reduced in the T-MH. Normal expression of *Nkx2.1* in the thyroid primordium was conserved in the *Rbpj*$^{-/-}$ embryos despite the developmental delay (Fig. 3D, asterisk). Notably, these *Rbpj*$^{-/-}$ embryos displayed hypoplasic forebrain vesicles (Fig. 3D, arrow).

These data suggested that, similar to the results in the chick embryos, NOTCH signalling was crucial to maintain the expression of *Shh* and thus *Nkx2.1* in the mouse AH. These data showed that the specific regulation of *Shh* expression by NOTCH in the AH was conserved between the chick and mouse embryos.

Conditional inhibition of the NOTCH pathway leads to telencephalic hypoplasia

We hypothesised that *Rbpj*$^{-/-}$ embryos that did not express *Shh* in the AH would subsequently exhibit a phenotype that was characteristic of a specific loss of *Shh* function in the AH. Mice with a specific loss of *Shh* function in the hypothalamus primordium were previously generated (9, 11). These mice displayed a particular phenotype with an abnormal hypothalamus and hypoplasic telencephalon. Despite the hypoplasic forebrain we observed in E9.5 *Rbpj*$^{-/-}$ embryos (Fig. 3D, arrow), further observation of the developing forebrain was compromised in these *Rbpj* knockout embryos as they are dying at this stage from heart failure (30). Therefore, to attempt a rescue of these dying embryos, we used *Rbpj*$^{L/L}$*;CreER*^{T2} mice where the activity of the Cre-recombinase could be induced at a specific time point during pregnancy using tamoxifen (24). *Rbpj*$^{L/L}$ excision was fully efficient 12 hours after the tamoxifen injection (Fig. S3; (29). This allowed us to excise the *Rbpj* gene and thus inhibit the NOTCH signalling pathway at a chosen developmental stage, before the establishment of NOTCH in the AH. NOTCH activity was first detected in the mouse prospective hypothalamus at E8.5 (43). Therefore, injection of 4 mg of tamoxifen was first done at E7.5 to get an inhibition of NOTCH by E8. However, treatment at this age induced morphological anomalies reminiscent to the *Rbpj*$^{-/-}$ embryo phenotypes. This included a shortening of the antero-posterior axis and lethality at E9.5. Therefore, we were not able to obtain a rescue of the heart phenotype when the embryos were treated with tamoxifen at E7.5 (Table S1 and Fig. S4; (29).

Therefore, similar to the treatment of the chick embryos with DAPT, we performed tamoxifen injections at various embryonic stages. When the pregnant mice were treated with tamoxifen at E7.75, *Rbpj*$^{L/L}$*;CreER*^{T2} embryos collected at E9.5 had an apparent similar morphology compared to the control *Rbpj*$^{L/L}$ (Fig. 4A and Fig. S4; (29). Genotypic analysis of embryos between E9.5 and E11.5 revealed no statistical deviation from the expected Mendelian ratios (Table S1; (29). However, by

E12.5, we were unable to harvest live *Rbpj*$^{L/L}$;*CreER*^{T2} embryos. Therefore, by treating embryos at E7.75 with 4 mg tamoxifen, we have only partially rescued the early lethality caused by a complete loss of NOTCH signalling.

In order to evaluate the effect of this conditional inactivation on the developing hypothalamus, we analysed the expression of *Nkx2.1* at E9.5. We observed half (n=4/8) of the *Rbpj*$^{L/L}$;*CreER*^{T2} embryos treated at E7.75 had a specific downregulation of *Nkx2.1* in the AH (Fig. 4A). This was reminiscent to what we obtained with *Rbpj*$^{-/-}$ embryos. Importantly, these rescued embryos did not show the developmental delay that was characteristic of *Rbpj*$^{-/-}$ mutant. These embryos were thus partially rescued morphologically, but still displayed a molecular mispatterning in the AH. The delayed lethality in these conditional mutant mice gave us the opportunity to study the consequence of this mispatterning in older embryos. At E10.5, mRNA distribution of *Shh* in *Rbpj*$^{L/L}$;*CreER*^{T2} embryos (n=21) from the same litter was extremely variable (Fig. 4B). *Shh* expression in the ventral forebrain ranged from slightly downregulated to completely absent (Fig. 4B).

The embryos with no *Shh* expression in the AH always had a reduction in size of the telencephalic vesicles (n=9) (Fig. 4B, asterisk). The phenotypic and molecular variability we observed was likely to be due to when the tamoxifen was injected into the pregnant mice; embryos were not at exactly the same stage of development.

We have further taken advantage of these partially rescued embryos to test the expression of *Fgf10*, a marker specific for T-MH. *Fgf10* expression extended into the AH in mouse embryos with a specific AH deletion of *Shh* (9, 11). Similarly, in our conditional mouse model, *Rbpj*$^{L/L}$;*CreER*^{T2}, half of the E9.5 (n=5) embryos, had the expression domain of *Fgf10* clearly extended anteriorly (Fig. 4C, bracket). This analysis indicated an anterior expansion of the expression domain of a posterior hypothalamic marker in *Rbpj*$^{L/L}$;*CreER*^{T2} embryos similar to what was previously described for *Shh*

deficient mutants (9, 11). At E10.5, *Rbpj*$^{L/L}$;*CreER*^{T2} embryos (n=22) displayed various levels of growth retardation of the developing brain, from an apparent normal morphological brain to mild forebrain defects, corresponding to a reduction of the size of the telencephalic vesicles (Fig. 4B, asterisk). In order to assess the telencephalic hypoplasia of these embryos, we analysed *Bmp7* expression as normal expression was found dorsally in the telencephalic vesicles (44). By E11.5, the *Bmp7* expression domain in the telencephalon was severely reduced in half of the *Rbpj*$^{L/L}$;*CreER*^{T2} embryos (n=6/12) (Fig. 4D, bracket). We also observed that at E11.5 the telencephalic vesicles in the *Rbpj*$^{L/L}$;*CreER*^{T2} embryos that were reduced in size. This is also reminiscent to the phenotype of the mouse models with a specific loss of *Shh* function in the hypothalamus primordium (9, 11).

Altogether, these findings suggested that the conditional loss of NOTCH signalling from E7.75 caused a downregulation of *Shh* in the AH and thus a failure of the forebrain to develop properly. Interestingly, tamoxifen treatment 6 hours later at E8.0 produced no telencephalic vesicle hypoplasia and no effect on the expression of *Shh* at the level of the ventral forebrain (Fig. S4; (29). Thus, timing of tamoxifen treatment was crucial. This suggested, similar to the DAPT-treated chick embryos, that NOTCH signalling was implicated in the appropriate control of *Shh* expression in the AH domains during a narrow window of time, between E7.75 and E8.25.

NOTCH signalling cooperates with SHH for pituitary gland formation

To test the genetic interaction between the SHH and NOTCH signalling pathways in the mouse, we sought to explore the consequences of a partial downregulation of both pathways by genetically deleting one copy of *Shh* and one copy of *Rbpj* in mice.

Unlike, homozygous mutants, that were not viable, *Rbpj*$^{+/-}$ and *Shh*$^{+/-}$ heterozygous mutants have been described as phenotypically unremarkable relative to their control littermates (2, 30). In this study, double heterozygous *Shh*$^{+/-}$;*Rbpj*$^{+/-}$ mice were created by intercrossing *Shh*$^{+/-}$ *mice* and *Rbpj*$^{+/-}$ mice. These intercrosses produced offspring that were viable with no obvious phenotypes. Genotyping of E18.5 embryos and 3 week old mice revealed the expected mendelian mode of inheritance for all genotypes (Table S2; (29).

The embryos during early hypothalamic development appeared normal (data not shown). Therefore, we decided to investigate the morphology of a more advanced hypothalamus. When histological head sections of *Shh*$^{+/-}$;*Rbpj*$^{+/-}$ embryos (n=4) were analysed at E18.5 a number of mild phenotypes were observed (Fig. 5). Defects included a dysplasic pituitary gland as well as a remnant connection between the anterior part of the pituitary (the adenohypophyseal gland) and the oral ectoderm (Fig. 5C and Fig. S5; (29). We also analysed E18.5 *Shh*$^{+/-}$;*Rbpj*$^{+/-}$ skeletal preparations (n=20) and discovered a malformation of the sphenoid corresponding to an agenesis of the presphenoid bone and a fully penetrant opening at the level of the basisphenoid midline (Fig. 5F).

During normal development, the pituitary gland develops from the interaction of the infundibulum, a region of the hypothalamus, and the Rathke's pouch, a derivative of oral ectoderm (45-47). The formation of the sphenoid bone establishes a definitive barrier between the pituitary gland and oral cavity (Fig. 5). It is presumed that a deviation in the development of the pituitary gland interferes with closure of the basisphenoid bone leading to an abnormal fenestration along the midline (48). The resulting hole is called a buccohypophyseal canal, also named craniopharyngeal canal. In all mammals, this canal normally closes during the early stages of development after the link between the

Rathke's pouch and oral ectoderm has disappeared. This canal is an ancestral vertebrate trait that has been lost in mice and humans by modulation of SHH signalling (48). In the brain of E18.5 *Shh*$^{+/-}$*;Rbpj*$^{+/-}$ embryos, the pituitary gland normally located between the hypothalamus and the basisphenoid bone was misplaced into the nasopharyngeal cavity through an abnormal opening in the midline of the basisphenoid bone (Fig. 5C and Fig. S5; (29). This indicated that the sphenoid bone cartilage was unable to develop properly in these *Shh*$^{+/-}$*;Rbpj*$^{+/-}$ mutant mice. A foramen was also observed at the level of the basisphenoid midline in E18.5 *Shh*$^{+/-}$ (n=17) embryos, but never as large compared to *Shh*$^{+/-}$*;Rbpj*$^{+/-}$ mutants (Fig. 5E). Interestingly, these results suggested that the basisphenoid bone was the most sensitive tissue to *Shh* insufficiency.

These observations indicated that morphogenesis of the pituitary gland was impaired in *Shh*$^{+/-}$*;Rbpj*$^{+/-}$ mice which led to basisphenoid abnormalities. This phenotype was probably due to a cumulative impact of NOTCH and SHH insufficiency during brain development.

Loss of function mutations in GLI2, a transcription factor component of SHH signalling pathway, resulted in a variable loss of pituitary development in human patients in the absence of midline brain defects (49). We tested the expression of *Gli2* in mouse mutants deficient in SHH signalling pathway (*Shh*$^{-/-}$) and mutants deficient in NOTCH pathway (*Rbpj*$^{L/L}$*;CreER*^{T2}) at E9.5. We observed that *Gli2* was downregulated in both mutant embryos (Fig. S6; (29). These data suggest that the anomalies we observed in *Shh*$^{+/-}$*;Rbpj*$^{+/-}$ mutants were probably due to a Gli2 failure during pituitary development.

Recurrent oligogenic events involving SHH and NOTCH pathway components in patients with holoprosencephaly

These results prompted us to perform a targeted analysis of the NOTCH and SHH components in a large cohort of patients with holoprosencephaly. We address the possibility that HPE could arise from the combined effects of hypomorphic variants in several genes belonging to NOTCH and SHH pathways. One hundred and forty-one patients harbouring different HPE malformations (from alobar to microforms) were analysed with the medical exome panel (33). The clinical data of these patients are shown in an online repository (Fig. S7; 29). Based on the theory of oligogenism and accumulation of hypomorphic variants to induce HPE (50) variants with a frequency over 0.01 in the general population (based on databases frequencies) were excluded. Focusing on exonic non-synonymous variants, 31 patients had variants in NOTCH pathway genes, among which 23 harboured variants in both the NOTCH and SHH signalling pathways (Fig. 6). Interestingly, 70% of the patients with *NOTCH* and *SHH* variants presented microforms and some have disorders of the hypothalamic-pituitary axis or malformations associated with these disorders, as nasal aperture piriform stenosis (NAPS) (51).

Discussion

Dynamic domains of *Shh* expression patterns in the ventral forebrain and a misbalance in SHH activity can cause a large spectrum of midline defects of the forebrain (52, 53). Here, we show for the first time that the NOTCH signalling pathway is implicated in the control of *Shh* expression in the AH and is thus critical for early forebrain patterning and the occurrence of HPE-like defects.

The use of diverse model organisms to study forebrain development provides evidence that the molecular pathways regulating the development of the ventral forebrain are conserved from fish to mammals (5, 54, 55). This conservation provides the opportunity to address questions regarding the implication of NOTCH signalling in human disorders by using the chick and mouse models. A potential implication of NOTCH signalling in early forebrain patterning has already been suggested with *DLL1,* a NOTCH ligand, alterations in HPE patients (17, 18). In agreement with this, NOTCH signalling is present in the ventral forebrain of both chick and mouse embryos during a stage of development compatible with an implication in HPE pathology (23, 43, 56). However, the molecular mechanism by which the NOTCH signalling pathway might regulate early development of the ventral forebrain as well as the relationship between the SHH and NOTCH signalling pathways remained unknown. Our expression studies confirm an overlap in the expression of NOTCH components and SHH components in the ventral forebrain. These results suggest the two pathways could regulate each other to ensure the correct patterning of the AH.

It is well established in the chick embryo that, initially, *Shh* is expressed throughout the presumptive hypothalamus from HH7 (1-somite stage) to HH14 (22-somite stage) and, subsequently, *Shh* expression becomes specifically restricted to the AH (37). In the AH, Shh promotes an anterior fate of the tissue and neurogenesis (10). The AH is a region in which high SHH activity is needed and therefore the consequent developmental outcomes are even more dosage sensitive (9-11).

Our expression studies show that NOTCH activity is strictly found in the AH from HH10, which is compatible with a role for NOTCH in the establishment of the forebrain midline. Consistent with this, we demonstrate that NOTCH signalling is necessary to maintain *Shh* expression in the AH during a short time window, between HH9 and HH12 in chick and between E7.75 and E8.25 in mouse. These time windows correspond to the same developmental stages in both species and this developmental period is crucial for the specification of the forebrain midline. Thus, high NOTCH signalling in the diencephalon early in development is essential for hypothalamic specification as it maintains the two specific markers of ventral cells, *Shh* and *Nkx2.1*. The ventral fate of the forebrain is thus reduced when NOTCH activity is decreased.

How NOTCH signalling contributes to maintaining *Shh* expression in the AH during this period is not yet defined. However, we know that NOTCH signalling pathway plays a key role in cell fate choice during AH neurogenesis (23, 24) in balancing the number of progenitors cells with that of differentiating neurons (57). Our previous studies show that transient inhibition of NOTCH signalling during early hypothalamic development enhances neurogenesis in the AH. This means that inhibition of NOTCH signalling from HH10 causes a rapid decline in the expression of downstream NOTCH components (e.g. *Hes5*) leading to the upregulation of the proneural bHLH gene, *Ascl1,* followed by a precocious neurogenesis and an excessive number of progenitor cells differentiating into neurons (23, 24). Thus, NOTCH signalling, through the repression of *Ascl1*, is necessary in the AH to maintain anterior progenitor cells and suppress neuronal differentiation. Once the anterior progenitor cells of the AH differentiate into neurons, *Shh* is downregulated in these cells (10). These data suggest that inactivation of NOTCH signalling causes precocious differentiation of the anterior progenitor cells into neurons promoting a premature downregulation of *Shh,* and therefore also leading to a downregulation of *Nkx2.1* and *Ptch1* in the AH.

When NOTCH signalling is removed in the mouse embryo just before the onset of its activity in the AH, we observe a specific downregulation of *Nkx2.1* in the AH, an anterior expansion of *Fgf10,* and a reduction in the size of the telencephalic vesicles. As this phenotype is also a common occurrence in the AH-specific-*Shh*-deficient model (9, 11), we assume that it is the reduction in SHH signalling in the AH that might underlie the forebrain phenotype of $Rbpj^{L/L};CreER^{T2}$ embryos. Therefore, our observations provide molecular evidence to show NOTCH as another signalling pathway, among multiple (e.g. FGF, NODAL, BMP), implicated in HPE occurrence through the control of *Shh* expression (9-11, 19, 37, 58, 59). This has been confirmed by generating double heterozygous ($Shh^{+/-};Rbpj^{+/-}$) mice; as the persistent buccohypophyseal canal we observe in these mice is a marker of variation in the dosage of SHH during midline morphogenesis (48). The same anomalies we observe in this study, although associated with other severe anomalies, are present in $Gas1^{-/-}$ (60) and $Cdo^{-/-}$ (61) mutant mice, two membrane proteins that act as agonists of SHH signalling during development. This indicates that the phenotype present in $Shh^{+/-};Rbpj^{+/-}$ mice is probably due to a supplementary deficiency of SHH signalling during pituitary formation compared to the single heterozygous mutant $Shh^{+/-}$. These results support a lower threshold of NOTCH activity being sufficient to cause clinically significant abnormalities in mice with a genetic mutation in the *Shh* gene. They show how sensitive the pituitary development is to a subtle SHH deficiency.

Persistence of the buccohypophyseal canal and pituitary gland aplasia represents an abnormality that occurs in human HPE (62, 63). In these patients, Adenopituitary (aP) gland tissues are located subpharyngeally. Furthermore, the *sella turcica*, which provides room for the pituitary gland in the body of the sphenoid bone, is partly absent. In these cases, similar to $Shh^{+/-};Rbpj^{+/-}$ mice, it is presumed that a deviation in the development of the pituitary gland results in an abnormality of the *sella turcica* (62). This functional study shows how haploinsufficiency of the SHH and NOTCH signalling pathways may contribute to congenital hypopituitarism that is associated with a *sella turcica* defect. Therefore, a more detailed characterisation of this HPE-like animal model ($Shh^{+/-};Rbpj^{+/-}$) is important, as it is the first example of a living mouse models with these unique microsigns

of HPE. Further investigation of the *Shh*$^{+/-}$;*Rbpj*$^{+/-}$ adult mice will allow the evaluation of the impact of such anomalies on physiology (such as growth hormone concentration) and cranial growth. This will provide an excellent opportunity for understanding normal and abnormal development of the ventral midline and may ultimately aid in the treatment of patients displaying hypothalamo-pituitary dysfunction.

The severity of HPE defects ranges from the complete absence of midline structures to a single upper incisor. It is becoming increasingly clear that phenotypic heterogeneity of HPE is dependent of the level of diminution of SHH as well as the timing and location of this deficiency (11, 52, 64, 65). The earlier and higher the decrease of SHH activity occurs, the more severe the HPE defects will be. Here, we show that *Shh* expression is NOTCH-dependent in a specific area of the ventral brain, the AH, during the later phases of its development. At this stage, SHH secreted by the axial mesoderm underlying the neural plate has already initiated development of the ventral midline in the brain (3) and we know that even a total absence of SHH in the AH does not give rise to severe HPE (for example, an alobar form with cyclopia) (11, 52, 64). Therefore, the telencephalic hypoplasia we describe in these NOTCH-deficient mouse embryos represents a congenital brain anomaly with a manifestation that is later compared to severe HPE due to differences in the timing and location of SHH attenuation (11, 64). Thus, inhibition of NOTCH signalling in the AH alone during forebrain development cannot produce severe HPE, but only microforms such as abnormal hypothalamic-pituitary axis and microcephaly. This agrees with the recent identification of neurodevelopmental disorders apparently not typical to HPE but associated to haploinsufficiency of *DLL1*. In these patients, intellectual disability and variable brain malformations such as microcephaly occurs (66). This may indicate that variants in NOTCH component genes underlie some cases of HPE microform in humans and that such putative mutations might contribute to more severe forms of HPE when in combination with variants in other genes involved in midline development. Recent whole-exome sequencing approaches show that several variants in SHH-related genes collectively contribute to the HPE phenotype (12, 50, 67, 68). Here, several patients exhibiting HPE anomalies present

accumulation of rare variants in genes related to the NOTCH and SHH pathways. Moreover, a high proportion of these patients present specific phenotypes at the level of the pituitary. Another recent exome sequencing study show that the pituitary stalk interruption syndrome is due to more than one mutation in genes mostly associated with NOTCH and SHH pathways (Guo et al., 2017), suggesting similar synergy of compound mutations underline the pathogenesis. These findings should motivate targeted gene mapping for new HPE candidate genes in regulators of NOTCH pathways.

This functional study shows how haploinsufficiency of both the SHH and NOTCH signalling pathways may contribute to not only to HPE but also to congenital hypopituitarism. This study has clinical implications, as many cases are not yet fully explained by genetic testing (12, 69). Furthermore, these results illustrate the need for expansion of the current diagnosis criteria to better capture the full range of brain and facial dysmorphology in disorders related to SHH-deficiency.

Acknowledgements

We particularly thank all members of the Molecular Genetics Laboratory (CHU, Rennes) and of the research team "Genetics of Development-related pathologies" (UMR6290 CNRS, University Rennes 1) for their help and advice. We are grateful to Philippos Mourikis and Shahragim Tajbakhsh for providing the *Rbpj*$^{L/L}$;*R26*$^{mTmG+/-}$ mouse. We also thank the animal house platform ARCHE and the histopathology platform H2P2 (SFR Biosit, Rennes, France). The authors acknowledge the Centre de Ressources Biologiques (CRB) Santé of Rennes for managing patient samples. We would like to thank the families for their participation in the study, all clinicians who referred patients with midline cerebral anomalies, the eight CLAD (Centres Labellisés pour les Anomalies du Développement) within France that belong to FECLAD, French centers of prenatal diagnosis (CPDPN) and the SOFFOET for foetal cases, and the 'filière AnDDI-Rares'. We thank graphic designer, Alexia Moutel.

Funding

This work was supported by the Agence Nationale de la Recherche (grant ANR-12-BSV1-0007-01) and the Agence de la Biomedecine (AMP2016).

Competing interests

No competing interests declared

References

1. Lupo G, Harris WA, Lewis KE. Mechanisms of ventral patterning in the vertebrate nervous system. Nature reviews Neuroscience. 2006;7(2):103-14.

2. Chiang C, Litingtung Y, Lee E, Young KE, Corden JL, Westphal H, et al. Cyclopia and defective axial patterning in mice lacking Sonic hedgehog gene function. Nature. 1996;383(6599):407-13.

3. Dale JK, Vesque C, Lints TJ, Sampath TK, Furley A, Dodd J, et al. Cooperation of BMP7 and SHH in the induction of forebrain ventral midline cells by prechordal mesoderm. Cell. 1997;90(2):257-69.

4. Shimogori T, Lee DA, Miranda-Angulo A, Yang Y, Wang H, Jiang L, et al. A genomic atlas of mouse hypothalamic development. Nature neuroscience. 2010;13(6):767-75.

5. Xie Y, Dorsky RI. Development of the hypothalamus: conservation, modification and innovation. Development. 2017;144(9):1588-99.

6. Ware M, Dupé V, Schubert FR. Evolutionary Conservation of the Early Axon Scaffold in the Vertebrate Brain. Developmental dynamics : an official publication of the American Association of Anatomists. 2015;244(10):1202-14.

7. Alvarez-Bolado G, Paul FA, Blaess S. Sonic hedgehog lineage in the mouse hypothalamus: from progenitor domains to hypothalamic regions. Neural development. 2012;7:4.

8. Corman TS, Bergendahl SE, Epstein DJ. Distinct temporal requirements for Sonic hedgehog signaling in development of the tuberal hypothalamus. Development. 2018;145(21).

9. Carreno G, Apps JR, Lodge EJ, Panousopoulos L, Haston S, Gonzalez-Meljem JM, et al. Hypothalamic sonic hedgehog is required for cell specification and proliferation of LHX3/LHX4 pituitary embryonic precursors. Development. 2017;144(18):3289-302.

10. Fu T, Towers M, Placzek MA. Fgf10(+) progenitors give rise to the chick hypothalamus by rostral and caudal growth and differentiation. Development. 2017;144(18):3278-88.

11. Zhao L, Zevallos SE, Rizzoti K, Jeong Y, Lovell-Badge R, Epstein DJ. Disruption of SoxB1-dependent Sonic hedgehog expression in the hypothalamus causes septo-optic dysplasia. Developmental cell. 2012;22(3):585-96.

12. Dubourg C, Kim A, Watrin E, de Tayrac M, Odent S, David V, et al. Recent advances in understanding inheritance of holoprosencephaly. American journal of medical genetics Part C, Seminars in medical genetics. 2018;178(2):258-69.

13. Fallet-Bianco C. Neuropathology of holoprosencephaly. American journal of medical genetics Part C, Seminars in medical genetics. 2018;178(2):214-28.

14. Mercier S, Dubourg C, Garcelon N, Campillo-Gimenez B, Gicquel I, Belleguic M, et al. New findings for phenotype-genotype correlations in a large European series of holoprosencephaly cases. Journal of medical genetics. 2011;48(11):752-60.

15. Rosenfeld JA, Ballif BC, Martin DM, Aylsworth AS, Bejjani BA, Torchia BS, et al. Clinical characterization of individuals with deletions of genes in holoprosencephaly pathways by aCGH refines the phenotypic spectrum of HPE. Human genetics. 2010;127(4):421-40.

16. Weiss K, Kruszka PS, Levey E, Muenke M. Holoprosencephaly from conception to adulthood. American journal of medical genetics Part C, Seminars in medical genetics. 2018;178(2):122-7.

17. Dubourg C, Carré W, Hamdi-Rozé H, Mouden C, Roume J, Abdelmajid B, et al. Mutational Spectrum in Holoprosencephaly Shows That FGF is a New Major Signaling Pathway. Human mutation. 2016;37(12):1329-39.

18. Dupé V, Rochard L, Mercier S, Le Petillon Y, Gicquel I, Bendavid C, et al. NOTCH, a new signaling pathway implicated in holoprosencephaly. Human molecular genetics. 2011;20(6):1122-31.

19. McCabe MJ, Gaston-Massuet C, Tziaferi V, Gregory LC, Alatzoglou KS, Signore M, et al. Novel FGF8 mutations associated with recessive holoprosencephaly, craniofacial defects, and hypothalamo-pituitary dysfunction. The Journal of clinical endocrinology and metabolism. 2011;96(10):E1709-18.

20. Roessler E, Pei W, Ouspenskaia MV, Karkera JD, Velez JI, Banerjee-Basu S, et al. Cumulative ligand activity of NODAL mutations and modifiers are linked to human heart defects and holoprosencephaly. Molecular genetics and metabolism. 2009;98(1-2):225-34.

21. Mzoughi S, Di Tullio F, Low DHP, Motofeanu CM, Ong SLM, Wollmann H, et al. PRDM15 loss of function links NOTCH and WNT/PCP signaling to patterning defects in holoprosencephaly. Science advances. 2020;6(2):eaax9852.

22. Selkoe D, Kopan R. Notch and Presenilin: regulated intramembrane proteolysis links development and degeneration. Annual review of neuroscience. 2003;26:565-97. doi: 10.1146/annurev.neuro.26.041002.131334. PubMed PMID: 12730322.

23. Ratié L, Ware M, Barloy-Hubler F, Romé H, Gicquel I, Dubourg C, et al. Novel genes upregulated when NOTCH signalling is disrupted during hypothalamic development. Neural development. 2013;8:25.

24. Ware M, Hamdi-Rozé H, Le Friec J, David V, Dupé V. Regulation of downstream neuronal genes by proneural transcription factors during initial neurogenesis in the vertebrate brain. Neural development. 2016;11(1):22.

25. Aujla PK, Bogdanovic V, Naratadam GT, Raetzman LT. Persistent expression of activated notch in the developing hypothalamus affects survival of pituitary progenitors and alters pituitary structure. Developmental dynamics : an official publication of the American Association of Anatomists. 2015;244(8):921-34.

26. Han H, Tanigaki K, Yamamoto N, Kuroda K, Yoshimoto M, Nakahata T, et al. Inducible gene knockout of transcription factor recombination signal binding protein-J reveals its essential role in T versus B lineage decision. International immunology. 2002;14(6):637-45.

27. Badea TC, Wang Y, Nathans J. A noninvasive genetic/pharmacologic strategy for visualizing cell morphology and clonal relationships in the mouse. The Journal of neuroscience : the official journal of the Society for Neuroscience. 2003;23(6):2314-22.

28. Muzumdar MD, Tasic B, Miyamichi K, Li L, Luo L. A global double-fluorescent Cre reporter mouse. Genesis. 2007;45(9):593-605.

29. Hamdi-Rozé H, Ware M, Guyodo H, Rizzo A, Ratié L, Rupin M, et al. Disrupted hypothalamo-pituitary axis in association with reduced SHH underlies the pathogenesis of NOTCH-deficiency. Figshare 2020 Deposited 1 Avril 2020. https://doi.org/10.6084/m9.figshare.12059121.v1.

30. Oka C, Nakano T, Wakeham A, de la Pompa JL, Mori C, Sakai T, et al. Disruption of the mouse RBP-J kappa gene results in early embryonic death. Development. 1995;121(10):3291-301.

31. Hamburger V, Hamilton HL. A series of normal stages in the development of the chick embryo. Journal of morphology. 1951;88(1):49-92.

32. Dupé V, Lumsden A. Hindbrain patterning involves graded responses to retinoic acid signalling. Development. 2001;128(12):2199-208.

33. Okazaki T, Murata M, Kai M, Adachi K, Nakagawa N, Kasagi N, et al. Clinical Diagnosis of Mendelian Disorders Using a Comprehensive Gene-Targeted Panel Test for Next-Generation Sequencing. Yonago acta medica. 2016;59(2):118-25.

34. Houtgast EJ, Sima VM, Bertels K, Al-Ars Z. Hardware acceleration of BWA-MEM genomic short read mapping for longer read lengths. Computational biology and chemistry. 2018;75:54-64.

35. De Summa S, Malerba G, Pinto R, Mori A, Mijatovic V, Tommasi S. GATK hard filtering: tunable parameters to improve variant calling for next generation sequencing targeted gene panel data. BMC bioinformatics. 2017;18(Suppl 5):119.

36. Wang K, Li M, Hakonarson H. ANNOVAR: functional annotation of genetic variants from high-throughput sequencing data. Nucleic acids research. 2010;38(16):e164.

37. Manning L, Ohyama K, Saeger B, Hatano O, Wilson SA, Logan M, et al. Regional morphogenesis in the hypothalamus: a BMP-Tbx2 pathway coordinates fate and proliferation through Shh downregulation. Developmental cell. 2006;11(6):873-85.

38. Pera EM, Kessel M. Patterning of the chick forebrain anlage by the prechordal plate. Development. 1997;124(20):4153-62.

39. de la Pompa JL, Wakeham A, Correia KM, Samper E, Brown S, Aguilera RJ, et al. Conservation of the Notch signalling pathway in mammalian neurogenesis. Development. 1997;124(6):1139-48.

40. Cohen M, Kicheva A, Ribeiro A, Blassberg R, Page KM, Barnes CP, et al. Ptch1 and Gli regulate Shh signalling dynamics via multiple mechanisms. Nature communications. 2015;6:6709. doi: 10.1038/ncomms7709.

41. Jarriault S, Brou C, Logeat F, Schroeter EH, Kopan R, Israel A. Signalling downstream of activated mammalian Notch. Nature. 1995;377(6547):355-8.

42. Blaess S, Szabo N, Haddad-Tovolli R, Zhou X, Alvarez-Bolado G. Sonic hedgehog signaling in the development of the mouse hypothalamus. Frontiers in neuroanatomy. 2014;8:156.

43. Ware M, Hamdi-Rozé H, Dupé V. Notch signaling and proneural genes work together to control the neural building blocks for the initial scaffold in the hypothalamus. Frontiers in neuroanatomy. 2014;8:140.

44. Danesh SM, Villasenor A, Chong D, Soukup C, Cleaver O. BMP and BMP receptor expression during murine organogenesis. Gene expression patterns : GEP. 2009;9(5):255-65.

45. Alatzoglou KS, Dattani MT. Genetic forms of hypopituitarism and their manifestation in the neonatal period. Early human development. 2009;85(11):705-12.

46. Takuma N, Sheng HZ, Furuta Y, Ward JM, Sharma K, Hogan BL, et al. Formation of Rathke's pouch requires dual induction from the diencephalon. Development. 1998;125(23):4835-40.

47. Treier M, Gleiberman AS, O'Connell SM, Szeto DP, McMahon JA, McMahon AP, et al. Multistep signaling requirements for pituitary organogenesis in vivo. Genes & development. 1998;12(11):1691-704.

48. Khonsari RH, Seppala M, Pradel A, Dutel H, Clement G, Lebedev O, et al. The buccohypophyseal canal is an ancestral vertebrate trait maintained by modulation in sonic hedgehog signaling. BMC biology. 2013;11:27.

49. Roessler E, Du YZ, Mullor JL, Casas E, Allen WP, Gillessen-Kaesbach G, et al. Loss-of-function mutations in the human GLI2 gene are associated with pituitary anomalies and holoprosencephaly-like features. Proceedings of the National Academy of Sciences of the United States of America. 2003;100(23):13424-9.

50. Kim A, Savary C, Dubourg C, Carre W, Mouden C, Hamdi-Roze H, et al. Integrated clinical and omics approach to rare diseases: novel genes and oligogenic inheritance in holoprosencephaly. Brain : a journal of neurology. 2019;142(1):35-49.

51. Guilmin-Crepon S, Garel C, Baumann C, Bremond-Gignac D, Bailleul-Forestier I, Magnier S, et al. High proportion of pituitary abnormalities and other congenital defects in children with congenital nasal pyriform aperture stenosis. Pediatric research. 2006;60(4):478-84.

52. Lipinski RJ, Holloway HT, O'Leary-Moore SK, Ament JJ, Pecevich SJ, Cofer GP, et al. Characterization of subtle brain abnormalities in a mouse model of Hedgehog pathway antagonist-induced cleft lip and palate. PloS one. 2014;9(7):e102603.

53. Marcucio RS, Cordero DR, Hu D, Helms JA. Molecular interactions coordinating the development of the forebrain and face. Developmental biology. 2005;284(1):48-61.

54. Grinblat Y, Lipinski RJ. A forebrain undivided: Unleashing model organisms to solve the mysteries of holoprosencephaly. Developmental dynamics : an official publication of the American Association of Anatomists. 2019;248(8):626-33.

55. Masek J, Andersson ER. The developmental biology of genetic Notch disorders. Development. 2017;144(10):1743-63.

56. Zhu X, Zhang J, Tollkuhn J, Ohsawa R, Bresnick EH, Guillemot F, et al. Sustained Notch signaling in progenitors is required for sequential emergence of distinct cell lineages during organogenesis. Genes & development. 2006;20(19):2739-53.

57. Cheung L, Le Tissier P, Goldsmith SG, Treier M, Lovell-Badge R, Rizzoti K. NOTCH activity differentially affects alternative cell fate acquisition and maintenance. eLife. 2018;7.

58. Davis SW, Camper SA. Noggin regulates Bmp4 activity during pituitary induction. Developmental biology. 2007;305(1):145-60.

59. Zhu X, Gleiberman AS, Rosenfeld MG. Molecular physiology of pituitary development: signaling and transcriptional networks. Physiological reviews. 2007;87(3):933-63.

60. Seppala M, Xavier GM, Fan CM, Cobourne MT. Boc modifies the spectrum of holoprosencephaly in the absence of Gas1 function. Biology open. 2014;3(8):728-40.

61. Cole F, Krauss RS. Microform holoprosencephaly in mice that lack the Ig superfamily member Cdon. Current biology : CB. 2003;13(5):411-5.

62. Kjaer I. Sella turcica morphology and the pituitary gland-a new contribution to craniofacial diagnostics based on histology and neuroradiology. European journal of orthodontics. 2015;37(1):28-36.

63. Kjaer I, Fischer-Hansen B. Human fetal pituitary gland in holoprosencephaly and anencephaly. Journal of craniofacial genetics and developmental biology. 1995;15(4):222-9.

64. Cordero D, Marcucio R, Hu D, Gaffield W, Tapadia M, Helms JA. Temporal perturbations in sonic hedgehog signaling elicit the spectrum of holoprosencephaly phenotypes. The Journal of clinical investigation. 2004;114(4):485-94.

65. Mercier S, David V, Ratie L, Gicquel I, Odent S, Dupe V. NODAL and SHH dose-dependent double inhibition promotes an HPE-like phenotype in chick embryos. Disease models & mechanisms. 2013;6(2):537-43.

66. Fischer-Zirnsak B, Segebrecht L, Schubach M, Charles P, Alderman E, Brown K, et al. Haploinsufficiency of the Notch Ligand DLL1 Causes Variable Neurodevelopmental Disorders. American journal of human genetics. 2019.

67. Hong M, Srivastava K, Kim S, Allen BL, Leahy DJ, Hu P, et al. BOC is a modifier gene in holoprosencephaly. Human mutation. 2017;38(11):1464-70.

68. Mouden C, Dubourg C, Carre W, Rose S, Quelin C, Akloul L, et al. Complex mode of inheritance in holoprosencephaly revealed by whole exome sequencing. Clinical genetics. 2016;89(6):659-68.

69. Gregory LC, Alatzoglou KS, McCabe MJ, Hindmarsh PC, Saldanha JW, Romano N, et al. Partial Loss of Function of the GHRH Receptor Leads to Mild Growth Hormone Deficiency. The Journal of clinical endocrinology and metabolism. 2016;101(10):3608-15.

Legends

Figure 1: SHH and NOTCH activity in the chick anterior hypothalamus

Comparison of *Nkx2.1*, *Hes5 and Ptch1* expression in the prospective hypothalamus (H), through either single labelling (B,C) or double labelling (A,D). The dotted lines delimit the anterior hypothalamus (AH) with the tubero-mamillary hypothalamus (T-MH). (E) Schematic of HH10 embryo showing expression domains of *Hes5*, *Ptch1*, *Nkx2.1* and *Shh* (37) in the developing hypothalamus. Mb, midbrain; OV, optic vesicles

Figure 2: The identity of the anterior hypothalamic was lost in DAPT-treated chick embryos

A comparison of gene expression in embryos after 16 hours of roller culture with DMSO (control) and DAPT at HH9. (A, B) Expression of *Shh* transcripts were detected in the anterior hypothalamus (AH) and tubero-mamillary hypothalamus (T-MH) in the control embryos, but was completely undetectable in the AH in embryos treated with DAPT at HH9 (arrowhead). (B) A ventral view of the dissected neural tube. (C,D) *Ptch1* and *Nkx2.1* expression was also lost in the AH of DAPT-treated embryos (arrowhead in C,D). Fb, forebrain; E, endoderm; Ov, optic vesicle.

Figure 3: Defective expression of *Shh* and *Nkx2.1* in the ventral forebrain of *Rbpj*$^{-/-}$ mouse mutants

Whole-mount *in situ* hybridisation analysis of *Shh* and *Nkx2.1* expression in mouse embryos. (A,C) *Shh* expression at E9.0 and (B,D) *Nkx2.1* expression at E9.5; *Shh* and *Nkx2.1* expression in the ventral forebrain was absent in *Rbpj*$^{-/-}$ (arrowheads). Brackets (A-B) designate the prospective hypothalamus (H) and its antero-posterior domains, anterior (AH) and tubero-mamillary (T-MH) domains. Asterisks

(B,D) indicate the thyroid primordium. The arrow in D indicates forebrain hypoplasia in *Rbpj*$^{-/-}$ mutants. Fb, forebrain; Ot, otic vesicle.

Figure 4: Forebrain hypoplasia in *Rbpj*$^{L/L}$;*CreER*^{T2} embryos

Rbpj$^{L/L}$ and *Rbpj*$^{L/L}$;*CreER*^{T2} tamoxifen-treated embryos at E7.75. Whole-mount *in situ* hybridisation analysis of *Nkx2.1, Shh, Fgf10 and BMP7* in embryos of the indicated genotype and stage (A D). (A), *Nkx2.1* mRNA was absent in the AH of the mutant embryo (arrowhead). (B), Expression of Shh was variable in mutant embryos are from the same litter. Asterisk indicates hypoplasic telencephalic vesicle. (C), *Fgf10* expression was restricted (bracket) in the tubero-mamillary hypothalamus (T-MH) in the control embryo (*Rbpj*$^{L/L}$). In the mutant embryo (*Rbpj*$^{L/L}$;*CreER*^{T2} *Fgf10* expression was expanded in a more anterior region of the hypothalamus (large bracket). (D), *Bmp7* expression in the telencephalic vesicles (bracket). AH, anterior hypothalamus; H, hypothalamus, Ot, otic vesicle; OV, optic vesicle; T, telencephalic vesicle.

Figure 5: Brain and cranial bone defects were observed in *Shh*$^{+/-}$;*Rbpj*$^{+/-}$ mutant embryos

(A-C) Hematoxylin and eosin staining of frontal section through E18.5 heads. Note the remnant connection (yellow arrow) between the anterior part of the pituitary gland and the oral ectoderm (OE). (D-F) Ventral views of cranial preparations of E18.5 embryos stained with Alizarin red and Alcian blue for bone and cartilage, respectively. Mandibles have been removed for visualisation. (E) White arrow indicates the persistent buccohypophyseal canal at the level of the midline in *Shh*$^{+/-}$ mutants. (F) Asterisk indicates the enlarged canal in Shh$^{+/-}$;Rbpj$^{+/-}$ basisphenoid. 3V, third ventricle; BS, basisphenoid; H, hypothalamus; OC, otic capsule; P, pituitary gland; PS, presphenoid; PX, pharynx.

Figure 6: Gene categories in two pathways corresponding to each patient applied to the medical exome panel. Twenty-three patients out of 141 had variants in both NOTCH and SHH signalling pathways.

Figure 1

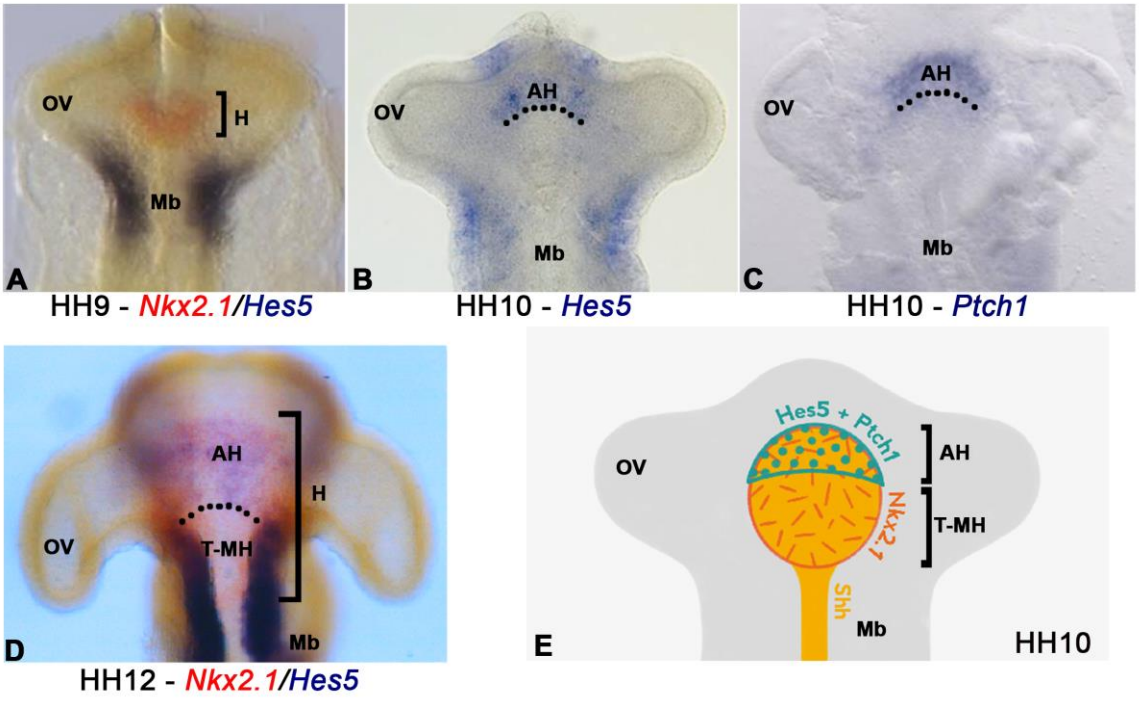

Figure 2

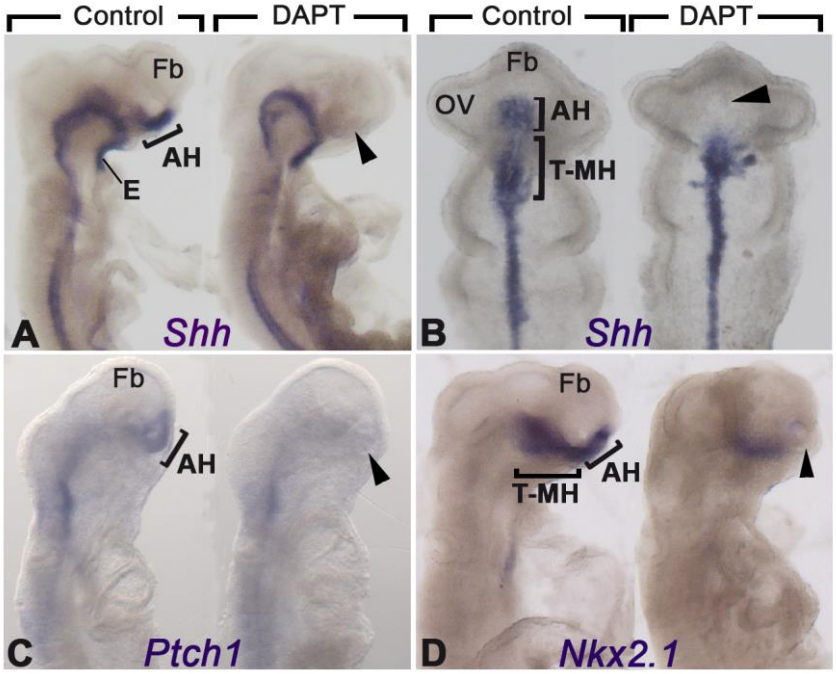

Figure 3

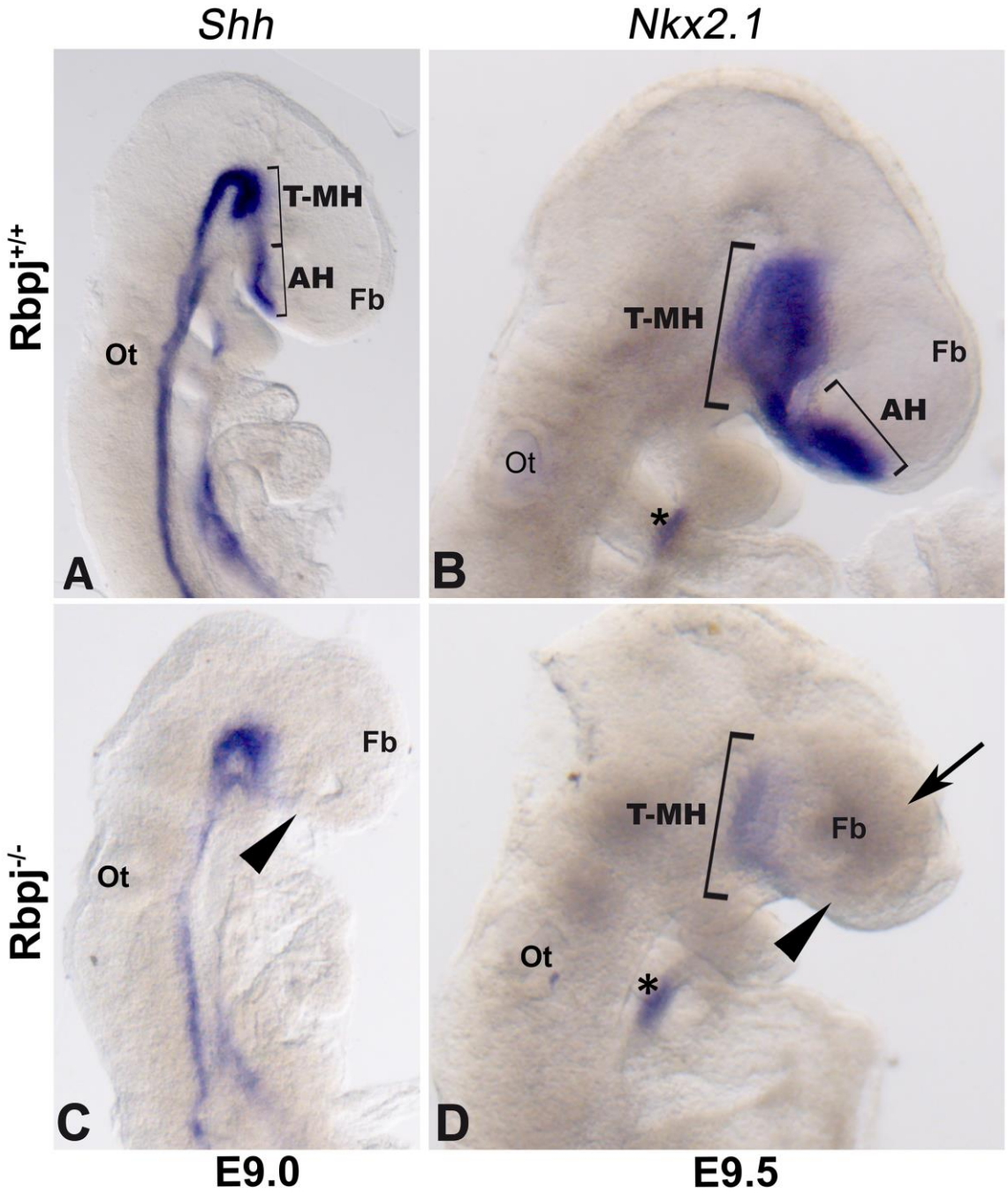

Figure 4

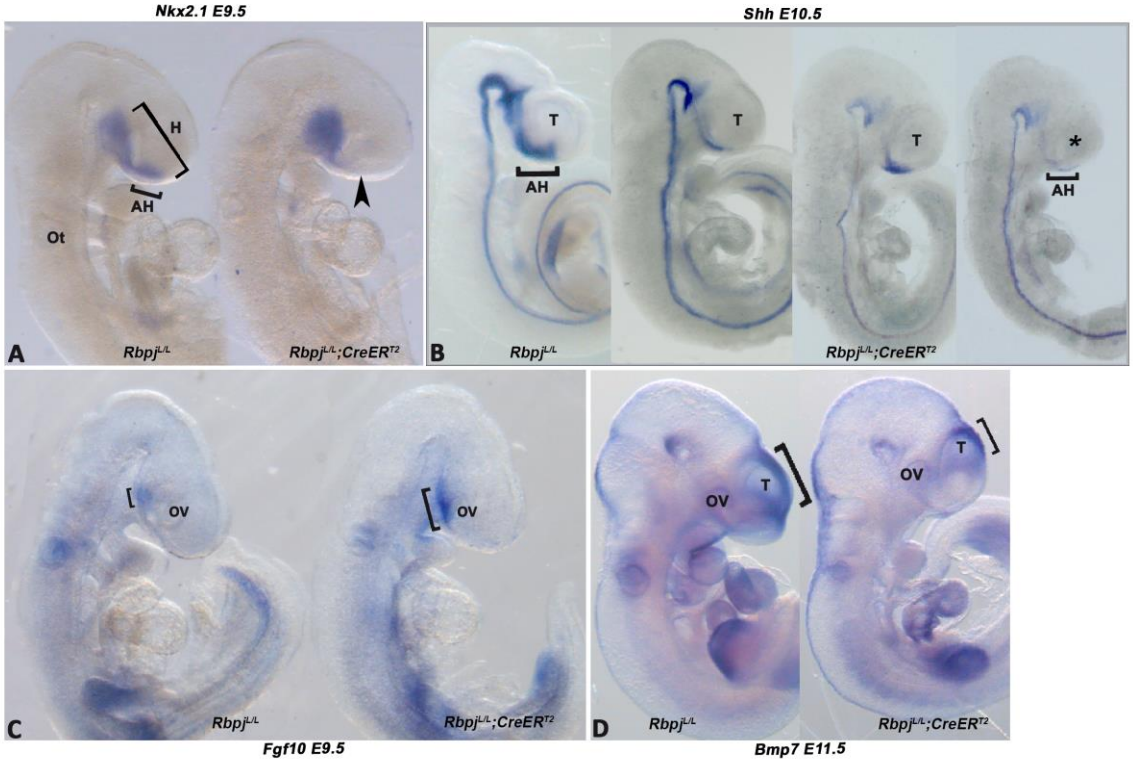

Figure 5

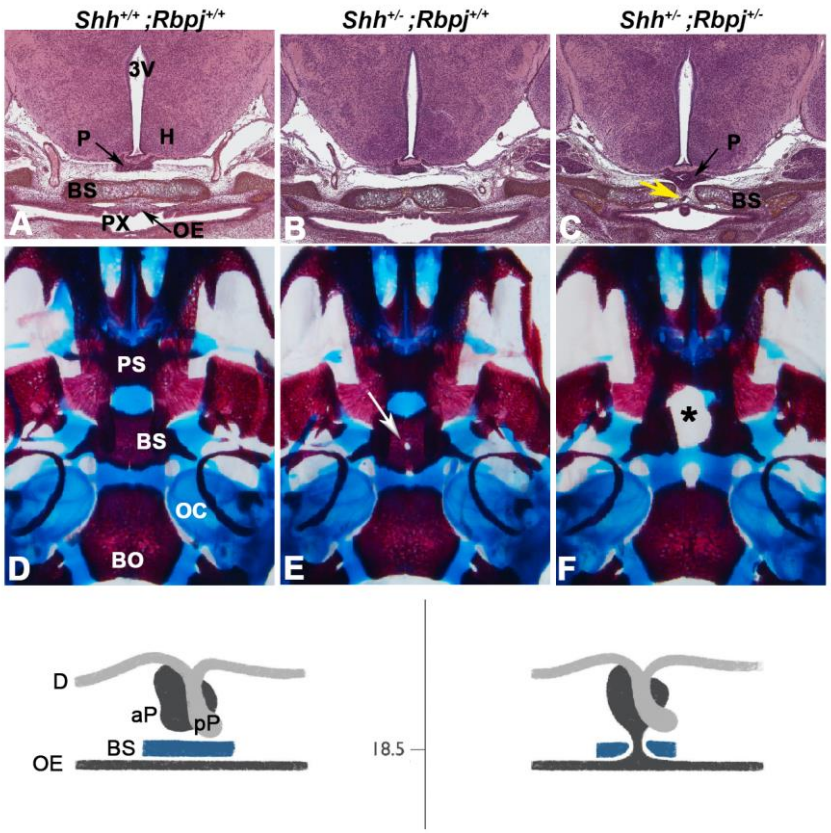

Figure 6